Minimum Rate Maximization for Wireless Powered Cloud Radio Access Networks

Jaein Kim, Hoon Lee, Seok-Hwan Park, and Inkyu Lee, *Fellow, IEEE*

***Abstract*—This paper studies the optimization of signal processing strategies for downlink and uplink of a cloud radio access network (C-RAN) that serves wireless powered users with non-linear energy harvesting (EH) circuits. On the downlink, a baseband processing unit (BBU) sends radio frequency signals to the users through a set of remote radio heads (RRHs), which is centrally managed by the BBU via finite-fronthaul links. Then, each user splits the received signal for information decoding and EH by utilizing the power splitting circuit. By using the harvested energy, each user communicates with the BBU via the RRHs on the uplink. In this paper, we tackle a problem of maximizing the minimum uplink rate of the users subject to the minimum downlink rate constraint as well as the per-node transmit power and fronthaul capacity constraints. To overcome the non-convexity of the problem, we propose an iterative algorithm based on a successive convex approximation method, which obtains a locally optimal solution. Numerical results confirm the effectiveness of the proposed techniques for C-RAN systems with battery-limited users.**

***Index Terms*—C-RAN, multiple antenna techniques, wireless power transfer.**

I. Introduction

Cloud radio access network (C-RAN) has been conceived as a promising architecture for future wireless systems, owing to its advantages of lowering operational expenditures and improving spectral efficiency [1]–[4]. This is enabled by migrating the baseband processing functionalities, which have been carried out by local base stations (BSs) in traditional cellular systems, to a baseband processing unit (BBU) connected to the BSs through fronthaul links [1], [2]. Since the BSs in the C-RAN perform only radio frequency (RF) functionalities, they are often referred to as remote radio heads (RRHs).

In the meantime, energy harvesting (EH) utilizing RF signals has been considered as a cost-effective method for extending the life time of wireless devices [5]–[13]. Wireless communication systems that leverage the EH methods are generally classified into two techniques: simultaneous wireless information and power transfer (SWIPT) [5], [6] and wireless powered communication network (WPCN) [7]–[10]. In the SWIPT systems, information and energy can be simultaneously transmitted at the same time and frequency band, while those operations are separately conducted in the WPCN systems. Specifically, on a downlink of the WPCN, each user equipment (UE) harvests the energy of RF signals transmitted from a hybrid access point (H-AP). Then, the UE exploits the harvested energy to communicate with the H-AP on a subsequent uplink of the WPCN. Recently, the C-RAN systems which utilize these EH methods have been studied in many literatures. For instance, in [14], [15], the energy-throughput tradeoff was investigated for a C-RAN system with the SWIPT capability. The authors in [16] considered a joint beamforming design to balance the fronthaul workload for a wireless powered C-RAN.

Most of the works on EH techniques in [5]–[16] prescribed a linear EH model, where the amount of the stored energy is modeled as a linear function of the received RF power. However, in practice, the EH circuits that process the RF signals exhibit a non-linear characteristic with respect to the input power level [17], [18]. To reflect practical non-linear EH properties, a non-linear EH model was proposed in [19] and the SWIPT and WPCN systems were studied in [19] and [20] under the non-linear EH models, respectively.

In this paper, we consider a wireless powered C-RAN system under a non-linear EH model, which has not yet been investigated in the literature. Assuming that the UEs have EH capabilities, each UE splits the received signal for information decoding (ID) and EH. We aim at jointly optimizing the downlink precoding, the uplink power control, the fronthaul quantization strategies, and the power splitting (PS) with the criterion of maximizing the minimum uplink rate of the UEs. In the optimization process, we impose the minimum downlink rate constraint as well as the per-node transmit power and fronthaul capacity constraints.

Since the overall performance is dependent on the time allocation on the downlink and uplink operations, the time allocation factor is also optimized. We tackle the formulated non-convex problem by adopting a successive convex approximation (SCA) approach [12]. To this end, we propose appropriate convex bounds for non-convex functions.

The main contributions of the paper are as follows: First, we formulate the joint downlink and uplink optimization problem for a wireless powered C-RAN system based on a non-linear EH model. Second, to obtain a locally optimal solution by utilizing the SCA technique, we propose a convex approximation method for the original problem. Finally, numerical results are provided to demonstrate the advantages of the proposed algorithm compared to conventional schemes.

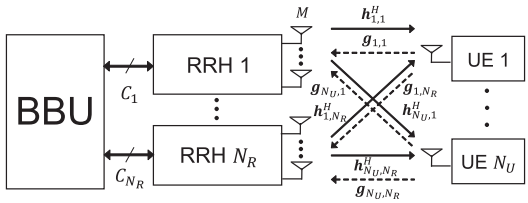

Fig. 1. Illustration of the downlink and uplink communications for a C-RAN system.

II. System Model

As shown in Fig. 1, we consider the downlink and uplink of a C-RAN system, where a BBU communicates with N_U single-antenna UEs through N_R RRHs, each equipped with M antennas. We define $\mathcal{N}_R \triangleq \{1, \ldots, N_R\}$ and $\mathcal{N}_U \triangleq \{1, \ldots, N_U\}$ as the sets of RRHs and UEs, respectively. We adopt an asymmetric time division duplex system, where the downlink and the uplink occupy τ and $1-\tau$ portions of the unit time resource block, respectively.

Manuscript received December 26, 2017; revised May 8, 2018 and October 15, 2018; accepted November 13, 2018. Date of publication November 19, 2018; date of current version January 15, 2019. This work was supported by the National Research Foundation (NRF) through the Ministry of Science, ICT and Future Planning, Korean Government, under Grant 2017R1A2B3012316. The review of this paper was coordinated by Dr. H. Zhu. *(Corresponding author: Inkyu Lee.)*

J. Kim and I. Lee are with the School of Electrical Engineering, Korea University, Seoul 02841, South Korea (e-mail: kji_07@korea.ac.kr; inkyu@korea.ac.kr).

H. Lee is with the Information Systems Technology and Design Pillar, Singapore University of Technology and Design, Singapore 487372 (e-mail: hoon_lee@sutd.edu.sg).

S.-H. Park is with the Division of Electronic Engineering, Chonbuk National University, Jeonju 54896, South Korea (e-mail: seokhwan@jbnu.ac.kr).

Color versions of one or more of the figures in this paper are available online at http://ieeexplore.ieee.org.

Digital Object Identifier 10.1109/TVT.2018.2881969

The received signal $y_k^{\rm dl} \in \mathbb{C}$ of UE $k \in \mathcal{N}_U$ on the downlink is given as

$$y_k^{\rm dl} = \sum_{i \in \mathcal{N}_R} \mathbf{h}_{k,i}^H \mathbf{x}_i^{\rm dl} + z_k^{\rm dl},$$

where $\mathbf{h}_{k,i} \in \mathbb{C}^{M\times 1}$ represents the downlink channel vector from RRH i to UE k, $\mathbf{a}^H$ denotes the Hermitian transpose of a vector $\mathbf{a}$, $\mathbf{x}_i^{\rm dl} \in \mathbb{C}^{M\times 1}$ is the transmit signal of RRH i with power constraint $\mathbb{E}\|\mathbf{x}_i^{\rm dl}\|^2 \le P_i^{\rm dl}$, and $z_k^{\rm dl} \sim \mathcal{CN}(0, \sigma_d^2)$ denotes the additive noise.

Also, the signal $\mathbf{y}_i^{\rm ul} \in \mathbb{C}^{M\times 1}$ received by RRH $i \in \mathcal{N}_R$ on the uplink is written as

$$\mathbf{y}_i^{\rm ul} = \sum_{k \in \mathcal{N}_U} \mathbf{g}_{k,i} x_k^{\rm ul} + \mathbf{z}_i^{\rm ul},$$

where $\mathbf{g}_{k,i} \in \mathbb{C}^{M\times 1}$ indicates the uplink channel vector from UE k to RRH i, $x_k^{\rm ul} \in \mathbb{C}$ stands for the signal transmitted by UE k, and $\mathbf{z}_i^{\rm ul} \in \mathbb{C}^{M\times 1} \sim \mathcal{CN}(\mathbf{0}, \sigma_u^2 \mathbf{I}_M)$ equals the additive noise. We impose that the signal $x_k^{\rm ul}$ is subject to an energy constraint $(1-\tau)\mathbb{E}|x_k^{\rm ul}|^2 \le E_k^{\rm ul} \triangleq E_{S,k}^{\rm ul} + E_{H,k}^{\rm ul}$, where $E_{S,k}^{\rm ul}$ is the energy provided by the storage of UE k, and $E_{H,k}^{\rm ul}$ represents the energy harvested by UE k from the downlink received signal, which will be detailed in the next section. We assume that RRH i is connected to the BBU through a fronthaul link of capacity C_i bps/Hz as in the standard C-RAN architecture (see, e.g., [1], [2]). Also, it is assumed that the fronthaul link is shared between the downlink and uplink directions so that, at each specific instance, it is used only for the downlink or uplink direction [21].

III. Proposed Wireless Powered C-RAN Systems

In this section, we describe the operations of the BBU, RRHs and UEs for the proposed wireless powered C-RAN system.

A. Downlink Communication

The BBU wishes to send messages $\{M_k^{\rm dl} \text{ for } k \in \mathcal{N}_U\}$ to the UEs on the downlink, where $M_k^{\rm dl} \in \{1, 2, \ldots, 2^{n R_k^{\rm dl}}\}$ defines the message intended for UE k with rate $R_k^{\rm dl}$ and block length n, which is assumed to be sufficiently large. For an effective management of inter-user interference on the downlink, the BBU performs linear precoding for each RRH as $\tilde{\mathbf{x}}_i^{\rm dl} = \sum_{k\in\mathcal{N}_U} \bar{\mathbf{v}}_{k,i} s_k^{\rm dl}$, where $\bar{\mathbf{v}}_{k,i} \in \mathbb{C}^{M\times 1}$ indicates the precoding vector for UE k at RRH i, and $s_k^{\rm dl} \sim \mathcal{CN}(0,1)$ denotes the baseband signal that encodes the message $M_k^{\rm dl}$. Note that multiplying a scalar $e^{j\phi_k}$ to $\bar{\mathbf{v}}_k$ does not change the performance regardless of ϕ_k [6], [12]. Therefore, without loss of optimality, we introduce new optimization variables $\mathbf{v}_{k,i}$ for $k \in \mathcal{N}_U$, $i \in \mathcal{N}_R$, where $\mathbf{v}_{k,i} = e^{-j\angle \mathbf{h}_k^H \bar{\mathbf{v}}_k} \bar{\mathbf{v}}_{k,i}$ with $\bar{\mathbf{v}}_k \triangleq [\bar{\mathbf{v}}_{k,1}^H \ldots \bar{\mathbf{v}}_{k,N_R}^H]^H$ and $\mathbf{h}_k \triangleq [\mathbf{h}_{k,1}^H \ldots \mathbf{h}_{k,N_R}^H]^H$.

To inform RRH i of the precoded signal $\tilde{\mathbf{x}}_i^{\rm dl}$ via the fronthaul link, the BBU produces the quantized signal $\mathbf{x}_i^{\rm dl}$ as $\mathbf{x}_i^{\rm dl} = \tilde{\mathbf{x}}_i^{\rm dl} + \mathbf{q}_i^{\rm dl}$ with the quantization noise $\mathbf{q}_i^{\rm dl} \sim \mathcal{CN}(\mathbf{0}, \mathbf{\Omega}_i^{\rm dl})$. RRH i can recover the signal $\mathbf{x}_i^{\rm dl}$ if the covariance matrix $\mathbf{\Omega}_i^{\rm dl}$ satisfies the condition [22]

$$g_i^{\rm dl}(\mathbf{v}, \mathbf{\Omega}_i^{\rm dl}) \triangleq I(\tilde{\mathbf{x}}_i^{\rm dl}; \mathbf{x}_i^{\rm dl}) = \Phi\bigg(\sum_{k\in\mathcal{N}_U} \mathbf{v}_{k,i}\mathbf{v}_{k,i}^H, \mathbf{\Omega}_i^{\rm dl}\bigg) \le C_i,$$

where $\mathbf{v} \triangleq \{\mathbf{v}_{k,i} \text{ for } k \in \mathcal{N}_U,\ i \in \mathcal{N}_R\}$ and $\Phi(\mathbf{A}, \mathbf{B}) \triangleq \log_2\det(\mathbf{A}+\mathbf{B}) - \log_2\det(\mathbf{B})$.

B. Power Splitting at UEs

By using the PS circuit with ratio $\alpha_k \in [0,1]$, UE k splits the received signal $y_k^{\rm dl}$ as the ID signal $y_{k,\rm dec}^{\rm dl} = \sqrt{\alpha_k} y_k^{\rm dl} + z_{C,k}$ and the EH signal $y_{k,\rm store}^{\rm dl} = \sqrt{1-\alpha_k} y_k^{\rm dl}$, where the noise $z_{C,k} \sim \mathcal{CN}(0, \sigma_C^2)$ is induced by a baseband circuitry [11, Sec. III-A].

1) Information Decoding: We assume that UE k decodes message $M_k^{\rm dl}$ based on the received signal $y_{k,\rm dec}^{\rm dl}$ by treating interference as the additive noise. As shown in [6], [12], $|\mathbf{h}_k^H \mathbf{v}_k|$ can be equivalently replaced by $\mathrm{Re}(\mathbf{h}_k^H \mathbf{v}_k)$ with the additional constraint $\mathrm{Re}(\mathbf{h}_k^H \mathbf{v}_k) \ge 0$, where $\mathbf{v}_k \triangleq [\mathbf{v}_{k,1}^H \ldots \mathbf{v}_{k,N_R}^H]^H$, and $\mathrm{Re}(z)$ represents the real part of $z \in \mathbb{C}$. Then, the rate $R_k^{\rm dl}$ is achievable if the following condition is fulfilled:

$$\begin{aligned} R_k^{\rm dl} &\le f_k^{\rm dl}(\mathbf{v}, \mathbf{\Omega}^{\rm dl}, \alpha_k, \tau) \\ &\triangleq \tau I(s_k^{\rm dl}; y_{k,\rm dec}^{\rm dl}) = \tau \log_2\left(1 + \frac{\alpha_k \mathrm{Re}(\mathbf{h}_k^H \mathbf{v}_k)^2}{\alpha_k \phi_k(\mathbf{v}, \mathbf{\Omega}^{\rm dl}) + \sigma_C^2}\right), \end{aligned}$$

where we define $\mathbf{\Omega}^{\rm dl} \triangleq \{\mathbf{\Omega}_i^{\rm dl} \text{ for } i \in \mathcal{N}_R\}$, and $\phi_k(\mathbf{v}, \mathbf{\Omega}^{\rm dl}) \triangleq \sum_{l\in\mathcal{N}_U\setminus\{k\}} |\mathbf{h}_k^H \mathbf{v}_l|^2 + \mathbf{h}_k^H \bar{\mathbf{\Omega}}^{\rm dl} \mathbf{h}_k + \sigma_d^2$ with $\bar{\mathbf{\Omega}}^{\rm dl} \triangleq \mathrm{diag}(\mathbf{\Omega}_1^{\rm dl}, \ldots, \mathbf{\Omega}_{N_R}^{\rm dl})$. To ensure downlink rate performance of UE k, we impose the minimum downlink rate constraint as $f_k^{\rm dl}(\mathbf{v}, \mathbf{\Omega}^{\rm dl}, \alpha_k, \tau) \ge R_{\rm min}^{\rm dl}$, where $R_{\rm min}^{\rm dl}$ indicates the required minimum downlink rate.

2) Energy Harvesting: Considering practical non-linear EH circuits, the harvested energy $E_{H,k}^{\rm ul}(\mathbf{v}, \mathbf{\Omega}^{\rm dl}, \alpha_k, \tau)$ at UE k utilizing the EH signal $y_{k,\rm store}^{\rm dl}$ on the downlink can be modeled as [19]

$$\begin{aligned} &E_{H,k}^{\rm ul}(\mathbf{v}, \mathbf{\Omega}^{\rm dl}, \alpha_k, \tau) \\ &\quad= \frac{\tau M_k}{1-\Pi_k}\left(\frac{1}{1+\exp\big(\delta_k(\epsilon_k - P_{H,k}^{\rm ul}(\mathbf{v}, \mathbf{\Omega}^{\rm dl}, \alpha_k))\big)} - \Pi_k\right), \end{aligned}$$

where M_k, δ_k and ϵ_k are the parameters obtained by a curve fitting tool, Π_k is denoted as $\Pi_k \triangleq 1/(1+\exp(\delta_k\epsilon_k))$ [19], [20], and $P_{H,k}^{\rm ul}(\mathbf{v}, \mathbf{\Omega}^{\rm dl}, \alpha_k) = \mathbb{E}|y_{k,\rm store}^{\rm dl}|^2 = (1-\alpha_k)(\mathrm{Re}\big(\mathbf{h}_k^H \mathbf{v}_k\big)^2 + \phi_k(\mathbf{v}, \mathbf{\Omega}^{\rm dl}))$ stands for the EH power.

C. Uplink Communication

On the uplink, UE k transmits message $M_k^{\rm ul} \in \{1, 2, \ldots, 2^{n R_k^{\rm ul}}\}$ of rate $R_k^{\rm ul}$ to the BBU. To this end, UE k encodes the message $M_k^{\rm ul}$ to produce the encoded baseband signal $s_k^{\rm ul} \sim \mathcal{CN}(0,1)$. Then, UE k obtains the transmit signal $x_k^{\rm ul}$ as $x_k^{\rm ul} = \rho_k s_k^{\rm ul}$, where $\rho_k \ge 0$ denotes the amplitude of $x_k^{\rm ul}$.

Since the fronthaul links have finite capacity, RRH i quantizes and compresses its received signal $\mathbf{y}_i^{\rm ul}$ as $\hat{\mathbf{y}}_i^{\rm ul} = \mathbf{y}_i^{\rm ul} + \mathbf{q}_i^{\rm ul}$, where $\mathbf{q}_i^{\rm ul} \sim \mathcal{CN}(\mathbf{0}, \mathbf{\Omega}_i^{\rm ul})$ represents the quantized noise signal [3]. Note that the quantized signal $\hat{\mathbf{y}}_i^{\rm ul}$ can be successfully decompressed at the BBU if the following condition is met

$$\begin{aligned} g_i^{\rm ul}(\boldsymbol{\rho}, \mathbf{\Omega}_i^{\rm ul}) &\triangleq I(\mathbf{y}_i^{\rm ul}; \hat{\mathbf{y}}_i^{\rm ul}) \\ &= \Phi\bigg(\sum_{k\in\mathcal{N}_U} \rho_k^2 \mathbf{g}_{k,i}\mathbf{g}_{k,i}^H + \sigma_u^2 \mathbf{I}_M, \mathbf{\Omega}_i^{\rm ul}\bigg) \le C_i, \end{aligned}$$

where $\boldsymbol{\rho} \triangleq \{\rho_k \text{ for } k \in \mathcal{N}_U\}$.

Based on the recovered signals $\{\hat{\mathbf{y}}_i^{\rm ul} \text{ for } i \in \mathcal{N}_R\}$, the BBU decodes the uplink messages $\{M_k^{\rm ul} \text{ for } k \in \mathcal{N}_U\}$ sent by the UEs with successive interference cancellation (SIC) decoding. For simplicity, we consider a fixed SIC order $1, 2, \ldots, N_U$, so that the uplink rate $R_k^{\rm ul}$ of UE k is bounded as

$$\begin{aligned} R_k^{\rm ul} &\le f_k^{\rm ul}(\boldsymbol{\rho}, \mathbf{\Omega}^{\rm ul}, \tau) \\ &\triangleq (1-\tau) I(s_k^{\rm ul}; \hat{\mathbf{y}}^{\rm ul}) = (1-\tau)\log_2(1+\rho_k^2 \mathbf{g}_k^H (\mathbf{\Phi}_k(\boldsymbol{\rho}, \mathbf{\Omega}^{\rm ul}))^{-1}\mathbf{g}_k)), \end{aligned}$$

where we define $\mathbf{\Omega}^{\rm ul} \triangleq \{\mathbf{\Omega}_i^{\rm ul} \text{ for } i \in \mathcal{N}_R\}$ and $\hat{\mathbf{y}}^{\rm ul} \triangleq \{\hat{\mathbf{y}}_i^{\rm ul} \text{ for } i \in \mathcal{N}_R\}$, $\mathbf{g}_k \triangleq [\mathbf{g}_{k,1}^H \ldots \mathbf{g}_{k,N_R}^H]^H$ and $\mathbf{\Phi}_k(\boldsymbol{\rho}, \mathbf{\Omega}^{\rm ul}) \triangleq \sum_{l\in\mathcal{N}_U > k} \rho_l^2 \mathbf{g}_l \mathbf{g}_l^H + \bar{\mathbf{\Omega}}^{\rm ul} + \sigma_u^2 \mathbf{I}_{MN_R}$, with $\bar{\mathbf{\Omega}}^{\rm ul} \triangleq \mathrm{diag}(\mathbf{\Omega}_1^{\rm ul}, \ldots, \mathbf{\Omega}_{N_R}^{\rm ul})$.

IV. Problem Description and Optimization

In this section, we address the problem of maximizing the minimum uplink rate of the UEs and propose an algorithm which finds a locally optimal solution to the problem.

A. Problem Description

We aim at maximizing the minimum uplink rate of the UEs, while satisfying the minimum downlink rate constraint as well as the per-node transmit power and the fronthaul capacity constraints. Here, the optimization variables are the downlink precoding vectors $\mathbf{v}$, the amplitudes of the uplink signals $\boldsymbol{\rho}$, the downlink and uplink fronthaul quantization noise covariance matrices $\{\boldsymbol{\Omega}^{\mathrm{dl}}, \boldsymbol{\Omega}^{\mathrm{ul}}\}$, the PS ratios $\boldsymbol{\alpha} \triangleq \{\alpha_k \text{ for } k \in \mathcal{N}_U\}$ and the time allocation factor τ. Then, the problem can be formulated as

$$\max_{\mathbf{v},\boldsymbol{\rho},\boldsymbol{\Omega}^{\mathrm{dl}},\boldsymbol{\Omega}^{\mathrm{ul}},\boldsymbol{\alpha},\tau} \quad \min_{k} \ f_k^{\mathrm{ul}}(\boldsymbol{\rho}, \boldsymbol{\Omega}^{\mathrm{ul}}, \tau) \tag{1a}$$

$$\text{s.t.} \quad f_k^{\mathrm{dl}}(\mathbf{v}, \boldsymbol{\Omega}^{\mathrm{dl}}, \alpha_k, \tau) \geq R_{\min}^{\mathrm{dl}},\ k \in \mathcal{N}_U, \tag{1b}$$

$$g_i^{\mathrm{ul}}(\boldsymbol{\rho}, \boldsymbol{\Omega}_i^{\mathrm{ul}}) \leq C_i,\ i \in \mathcal{N}_R, \tag{1c}$$

$$g_i^{\mathrm{dl}}(\mathbf{v}, \boldsymbol{\Omega}_i^{\mathrm{dl}}) \leq C_i,\ i \in \mathcal{N}_R, \tag{1d}$$

$$(1-\tau)\rho_k^2 \leq E_{S,k}^{\mathrm{ul}} + E_{H,k}^{\mathrm{ul}}(\mathbf{v}, \boldsymbol{\Omega}^{\mathrm{dl}}, \alpha_k, \tau),\ k \in \mathcal{N}_U, \tag{1e}$$

$$p_i^{\mathrm{dl}}(\mathbf{v}, \boldsymbol{\Omega}_i^{\mathrm{dl}}) \leq P_i^{\mathrm{dl}},\ i \in \mathcal{N}_R, \tag{1f}$$

$$\mathrm{Re}(\mathbf{h}_k^H \mathbf{v}_k) \geq 0,\ k \in \mathcal{N}_U, \tag{1g}$$

$$\tau \in [0,1],\ \alpha_k \in [0,1],\ k \in \mathcal{N}_U, \tag{1h}$$

where we define $p_i^{\mathrm{dl}}(\mathbf{v}, \boldsymbol{\Omega}_i^{\mathrm{dl}}) \triangleq \sum_{k \in \mathcal{N}_U} \mathbf{v}_{k,i}^H \mathbf{v}_{k,i} + \mathrm{tr}(\boldsymbol{\Omega}_i^{\mathrm{dl}})$. Problem (1) is non-convex due to the objective function (1a) and the constraints (1b)–(1e), and thus it is difficult to obtain the global optimal solution. In the next subsection, we present an iterative algorithm that obtains a locally optimal solution.

B. Proposed Optimization Algorithm

To solve the non-convex problem (1), we adopt the SCA approach [12] which successively approximates the original non-convex problem to a convex one. To this end, we first introduce new variables $\tilde{\mathbf{v}} \triangleq \{\tilde{\mathbf{v}}_k \text{ for } k \in \mathcal{N}_U\}$, $\tilde{\boldsymbol{\rho}} \triangleq \{\tilde{\rho}_k \text{ for } k \in \mathcal{N}_U\}$, $\tilde{\boldsymbol{\Omega}}^{\mathrm{dl}} \triangleq \{\tilde{\boldsymbol{\Omega}}_i^{\mathrm{dl}} \text{ for } i \in \mathcal{N}_R\}$ and $\tilde{\boldsymbol{\Omega}}^{\mathrm{ul}} \triangleq \{\tilde{\boldsymbol{\Omega}}_i^{\mathrm{ul}} \text{ for } i \in \mathcal{N}_R\}$, where $\tilde{\mathbf{v}}_k = \tau \mathbf{v}_k$, $\tilde{\rho}_k = (1-\tau)\rho_k$, $\tilde{\boldsymbol{\Omega}}_i^{\mathrm{dl}} = \tau \boldsymbol{\Omega}_i^{\mathrm{dl}}$ and $\tilde{\boldsymbol{\Omega}}_i^{\mathrm{ul}} = (1-\tau)\boldsymbol{\Omega}_i^{\mathrm{ul}}$, which make finding convex approximations of the non-convex functions in (1) tractable. Note that these new variables can be interpreted as energy variables in Joule, while the original ones have unit of Watt. In the following, we propose approximations of the non-convex functions in (1) by using the following inequalities

$$\ln(1+x^2 \mathbf{a}^H \mathbf{Y}^{-1} \mathbf{a}) \geq \psi_1(x, \mathbf{Y}, \mathbf{a}) \tag{2}$$
$$\triangleq \ln(1+(x^{(t)})^2 \mathbf{a}^H (\mathbf{Y}^{(t)})^{-1} \mathbf{a}) + (2x - x^{(t)}) x^{(t)} \mathbf{a}^H (\mathbf{Y}^{(t)})^{-1} \mathbf{a} - \mathrm{tr}((\mathbf{Y} + x^2 \mathbf{a}\mathbf{a}^H)((\mathbf{Y}^{(t)})^{-1} - (\mathbf{Y}^{(t)} + (x^{(t)})^2 \mathbf{a}\mathbf{a}^H)^{-1})),$$

$$\ln\left(1 + \frac{x^2}{y}\right) \geq \psi_2(x,y) \triangleq \ln\left(1 + \frac{(x^{(t)})^2}{y^{(t)}}\right) + \frac{(2x - x^{(t)})x^{(t)}}{y^{(t)}} - (x^2 + y)\left(\frac{1}{y^{(t)}} - \frac{1}{y^{(t)} + (x^{(t)})^2}\right), \tag{3}$$

$$\ln\det(\mathbf{Y}) \leq \psi_3(\mathbf{Y}) \triangleq \ln\det(\mathbf{Y}^{(t)}) + \mathrm{tr}(\mathbf{Y}(\mathbf{Y}^{(t)})^{-1}) - L, \tag{4}$$

$$\mathbf{a}^H \mathbf{a} \geq \psi_4(\mathbf{a}) \triangleq 2\mathrm{Re}((\mathbf{a}^{(t)})^H \mathbf{a}) - (\mathbf{a}^{(t)})^H \mathbf{a}^{(t)}, \tag{5}$$

for arbitrary variables $x \in \mathbb{R}$, $\mathbf{a} \in \mathbb{C}^{L \times 1}$, $\mathbf{Y} \in \mathbb{C}^{L \times L} \succ 0$, and $y > 0$, where $z^{(t)}$ denotes the quantity z obtained at the t-th iteration of the SCA. Note that the inequalities (2) and (3), (4), and (5) are derived by applying a similar approach in [12], [4] and [6], respectively.

1) Convex Bounds for (1a) and (1b): By using the inequalities (2) and (3), we consider lower bounds of $f_k^{\mathrm{ul}}(\boldsymbol{\rho}, \boldsymbol{\Omega}^{\mathrm{ul}}, \tau)$ in (1a) and $f_k^{\mathrm{dl}}(\mathbf{v}, \boldsymbol{\Omega}^{\mathrm{dl}}, \alpha_k, \tau)$ in (1b) as

$$f_k^{\mathrm{ul}}(\boldsymbol{\rho}, \boldsymbol{\Omega}^{\mathrm{ul}}, \tau) = f_k^{\mathrm{ul}}\left(\frac{\tilde{\boldsymbol{\rho}}}{1-\tau}, \frac{\tilde{\boldsymbol{\Omega}}^{\mathrm{ul}}}{1-\tau}, \tau\right) \geq \tilde{f}_k^{(t),\mathrm{ul}}(\tilde{\boldsymbol{\rho}}, \tilde{\boldsymbol{\Omega}}^{\mathrm{ul}}, \tau),$$

$$f_k^{\mathrm{dl}}(\mathbf{v}, \boldsymbol{\Omega}^{\mathrm{dl}}, \alpha_k, \tau) = f_k^{\mathrm{dl}}\left(\frac{\tilde{\mathbf{v}}}{\tau}, \frac{\tilde{\boldsymbol{\Omega}}^{\mathrm{dl}}}{\tau}, \alpha_k, \tau\right) \geq \bar{f}_k^{(t),\mathrm{dl}}(\tilde{\mathbf{v}}, \tilde{\boldsymbol{\Omega}}^{\mathrm{dl}}, \alpha_k, \tau), \tag{6}$$

where $\tilde{f}_k^{(t),\mathrm{ul}}(\tilde{\boldsymbol{\rho}}, \tilde{\boldsymbol{\Omega}}^{\mathrm{ul}}, \tau) \triangleq (1-\tau)\psi_1(\tilde{\rho}_k/(1-\tau), \boldsymbol{\Phi}_k(\tilde{\boldsymbol{\rho}}/(1-\tau), \tilde{\boldsymbol{\Omega}}^{\mathrm{ul}}/(1-\tau)), \mathbf{g}_k)/\ln 2$ and $\bar{f}_k^{(t),\mathrm{dl}}(\tilde{\mathbf{v}}, \tilde{\boldsymbol{\Omega}}^{\mathrm{dl}}, \alpha_k, \tau) \triangleq \tau\psi_2(\mathrm{Re}(\mathbf{h}_k^H \tilde{\mathbf{v}}_k)/\tau, \phi_k(\tilde{\mathbf{v}}/\tau, \tilde{\boldsymbol{\Omega}}^{\mathrm{dl}}/\tau) + \sigma_C^2/\alpha_k)/\ln 2$.

While $\tilde{f}_k^{(t),\mathrm{ul}}(\tilde{\boldsymbol{\rho}}, \tilde{\boldsymbol{\Omega}}^{\mathrm{ul}}, \tau)$ is a concave function, $\bar{f}_k^{(t),\mathrm{dl}}(\tilde{\mathbf{v}}, \tilde{\boldsymbol{\Omega}}^{\mathrm{dl}}, \alpha_k, \tau)$ is not concave due to coupled variables τ and α_k as τ/α_k in (6). To tackle this issue, we introduce an additional variable μ_k with $\mu_k \geq \tau/\alpha_k$. Equivalently, we have

$$\ln \mu_k \geq \ln \tau - \ln \alpha_k. \tag{7}$$

Then, by using μ_k, we express a concave lower bound of $\bar{f}_k^{(t),\mathrm{dl}}(\tilde{\mathbf{v}}, \tilde{\boldsymbol{\Omega}}^{\mathrm{dl}}, \alpha_k, \tau)$ given as

$$\bar{f}_k^{(t),\mathrm{dl}}(\tilde{\mathbf{v}}, \tilde{\boldsymbol{\Omega}}^{\mathrm{dl}}, \alpha_k, \tau) \geq \tilde{f}_k^{(t),\mathrm{dl}}(\tilde{\mathbf{v}}, \tilde{\boldsymbol{\Omega}}^{\mathrm{dl}}, \mu_k, \tau),$$

where we define the function $\tilde{f}_k^{(t),\mathrm{dl}}(\tilde{\mathbf{v}}, \tilde{\boldsymbol{\Omega}}^{\mathrm{dl}}, \mu_k, \tau) \triangleq \tau\psi_2(\mathrm{Re}(\mathbf{h}_k^H \tilde{\mathbf{v}}_k)/\tau, \phi_k(\tilde{\mathbf{v}}/\tau, \tilde{\boldsymbol{\Omega}}^{\mathrm{dl}}/\tau) + \sigma_C^2 \mu_k/\tau)/\ln 2$.

To address the non-convex constraint (7), based on the inequality (4), we adopt a convex upper bound of $\ln \tau$ given as $\ln \tau \leq \psi_3(\tau, \tau^{(t)})$. As a result, the minimum downlink rate constraint (1b) can be recast as the following convex constraint

$$\tilde{f}_k^{(t),\mathrm{dl}}(\tilde{\mathbf{v}}, \tilde{\boldsymbol{\Omega}}^{\mathrm{dl}}, \mu_k, \tau) \geq R_{\min}^{\mathrm{dl}},\ k \in \mathcal{N}_U, \tag{8}$$

with the additional constraint

$$\psi_3(\tau) - \ln \alpha_k \leq \ln \mu_k,\ k \in \mathcal{N}_U. \tag{9}$$

2) Convex Bounds for (1c) and (1d): By using the inequality (4), the functions $g_i^{\mathrm{ul}}(\boldsymbol{\rho}, \boldsymbol{\Omega}_i^{\mathrm{ul}})$ in (1c) and $g_i^{\mathrm{dl}}(\mathbf{v}, \boldsymbol{\Omega}_i^{\mathrm{dl}})$ in (1d) are respectively upper bounded by

$$g_i^{\mathrm{ul}}(\boldsymbol{\rho}, \boldsymbol{\Omega}_i^{\mathrm{ul}}) = g_i^{\mathrm{ul}}\left(\frac{\tilde{\boldsymbol{\rho}}}{1-\tau}, \frac{\tilde{\boldsymbol{\Omega}}_i^{\mathrm{ul}}}{1-\tau}\right) \leq \tilde{g}_i^{(t),\mathrm{ul}}(\tilde{\boldsymbol{\rho}}, \tilde{\boldsymbol{\Omega}}_i^{\mathrm{ul}}, \tau)$$
$$\triangleq \frac{1}{\ln 2}\psi_3\left(\sum_{k \in \mathcal{N}_U} \frac{\tilde{\rho}_k^2 \mathbf{g}_{k,i} \mathbf{g}_{k,i}^H}{(1-\tau)^2} + \frac{\tilde{\boldsymbol{\Omega}}_i^{\mathrm{ul}}}{1-\tau} + \sigma_u^2 \mathbf{I}_M\right) - \log_2 \det\left(\frac{\tilde{\boldsymbol{\Omega}}_i^{\mathrm{ul}}}{1-\tau}\right),$$

$$g_i^{\mathrm{dl}}(\mathbf{v}, \boldsymbol{\Omega}_i^{\mathrm{dl}}) = g_i^{\mathrm{dl}}\left(\frac{\tilde{\mathbf{v}}}{\tau}, \frac{\tilde{\boldsymbol{\Omega}}_i^{\mathrm{dl}}}{\tau}\right) \leq \tilde{g}_i^{(t),\mathrm{dl}}(\tilde{\mathbf{v}}, \tilde{\boldsymbol{\Omega}}_i^{\mathrm{dl}}, \tau)$$
$$\triangleq \frac{1}{\ln 2}\psi_3\left(\sum_{k \in \mathcal{N}_U} \frac{\tilde{\mathbf{v}}_{k,i} \tilde{\mathbf{v}}_{k,i}^H}{\tau^2} + \frac{\tilde{\boldsymbol{\Omega}}_i^{\mathrm{dl}}}{\tau}\right) - \log_2 \det\left(\frac{\tilde{\boldsymbol{\Omega}}_i^{\mathrm{dl}}}{\tau}\right).$$

Since $(1-\tau)\tilde{g}_i^{(t),\mathrm{ul}}(\tilde{\boldsymbol{\rho}}, \tilde{\boldsymbol{\Omega}}_i^{\mathrm{ul}}, \tau)$ and $\tau \tilde{g}_i^{(t),\mathrm{dl}}(\tilde{\mathbf{v}}, \tilde{\boldsymbol{\Omega}}_i^{\mathrm{dl}}, \tau)$ are convex functions, the uplink and downlink fronthaul capacity constraints in (1c) and (1d) can be respectively approximated as the following convex constraints

$$(1-\tau)\tilde{g}_i^{(t),\mathrm{ul}}(\tilde{\boldsymbol{\rho}}, \tilde{\boldsymbol{\Omega}}_i^{\mathrm{ul}}, \tau) \leq (1-\tau)C_i,\ i \in \mathcal{N}_R, \tag{10}$$

$$\tau \tilde{g}_i^{(t),\mathrm{dl}}(\tilde{\mathbf{v}}, \tilde{\boldsymbol{\Omega}}_i^{\mathrm{dl}}, \tau) \leq \tau C_i,\ i \in \mathcal{N}_R. \tag{11}$$

3) Convex Bound for (1e): In order to handle the non-convex constraint in (1e), which is equivalently expressed as

$$\frac{\tilde{\rho}_k^2}{1-\tau} \leq E_{S,k}^{\mathrm{ul}} + E_{H,k}^{\mathrm{ul}}\left(\frac{\tilde{\mathbf{v}}}{\tau}, \frac{\tilde{\boldsymbol{\Omega}}^{\mathrm{dl}}}{\tau}, \alpha_k, \tau\right),\ k \in \mathcal{N}_U, \tag{12}$$

we introduce new optimization variables $\boldsymbol{e} \triangleq \{e_k \geq 0 \text{ for } k \in \mathcal{N}_U\}$ and $\boldsymbol{\theta} \triangleq \{\theta_k \geq 0 \text{ for } k \in \mathcal{N}_U\}$ subject to the non-convex constraints

$$\ln e_k \leq \ln \frac{\tau M_k}{(1-\Pi_k)(1+\exp(\delta_k(\epsilon_k-\theta_k)))}, \; k \in \mathcal{N}_U, \tag{13}$$

$$\theta_k \leq P_{H,k}^{\text{ul}}\left(\frac{\tilde{\mathbf{v}}}{\tau}, \frac{\tilde{\boldsymbol{\Omega}}^{\text{dl}}}{\tau}, \alpha_k\right), \; k \in \mathcal{N}_U. \tag{14}$$

From (13) and (14), the per-UE transmit power constraint (12) is approximated as the following convex constraint

$$\frac{\tilde{\rho}_k^2}{1-\tau} \leq E_{S,k}^{\text{ul}} + e_k - \frac{\tau M_k \Pi_k}{1-\Pi_k}, \; k \in \mathcal{N}_U. \tag{15}$$

Also, the constraint (14) can be equivalently expressed as

$$\ln \tau + \ln \theta_k \leq \ln\left(\tau P_{H,k}^{\text{ul}}\left(\frac{\tilde{\mathbf{v}}}{\tau}, \frac{\tilde{\boldsymbol{\Omega}}^{\text{dl}}}{\tau}, \alpha_k\right)\right), \; k \in \mathcal{N}_U. \tag{16}$$

Since (13) and (16) are non-convex constraints, by using the inequalities (4) and (5), the convex constraints of (13) and (16) are respectively obtained as

$$\psi_3(e_k) \leq \ln \frac{\tau M_k}{(1-\Pi_k)(1+\exp(\delta_k(\epsilon_k-\theta_k)))}, k \in \mathcal{N}_U, \tag{17}$$

$$\psi_3(\tau) + \psi_3(\theta_k) \leq \ln(1-\alpha_k) + \ln\left(\tilde{P}_{H,k}^{(t),\text{ul}}(\tilde{\mathbf{v}}, \tilde{\boldsymbol{\Omega}}^{\text{dl}}, \tau)\right), \; k \in \mathcal{N}_U, \tag{18}$$

where $\tilde{P}_{H,k}^{(t),\text{ul}}(\tilde{\mathbf{v}}, \tilde{\boldsymbol{\Omega}}^{\text{dl}}, \tau) \triangleq \sum_{l \in \mathcal{N}_U \setminus \{k\}} \tau\psi_4(\mathbf{h}_k^H \tilde{\mathbf{v}}_l/\tau) + \tau\psi_4(\text{Re}(\mathbf{h}_k^H \tilde{\mathbf{v}}_k)/\tau) + \mathbf{h}_k^H \tilde{\bar{\boldsymbol{\Omega}}}^{\text{dl}} \mathbf{h}_k + \tau\sigma_d^2$ with $\tilde{\bar{\boldsymbol{\Omega}}}^{\text{dl}} \triangleq \text{diag}(\tilde{\boldsymbol{\Omega}}_1^{\text{dl}}, \ldots, \tilde{\boldsymbol{\Omega}}_{N_R}^{\text{dl}})$.

4) Convex Problem: Based on the above results, we can formulate the convex approximation problem of the original problem (1) as

$$\max_{\mathcal{A}} \min_{k} \quad \tilde{f}_k^{(t),\text{ul}}(\tilde{\boldsymbol{\rho}}, \tilde{\boldsymbol{\Omega}}^{\text{ul}}, \tau) \tag{19a}$$

$$\text{s.t.} \quad e_k \geq 0, \; k \in \mathcal{N}_U, \tag{19b}$$

$$\theta_k \geq 0, \; k \in \mathcal{N}_U, \tag{19c}$$

$$\tau p_i^{\text{dl}}\left(\frac{\mathbf{v}}{\tau}, \frac{\boldsymbol{\Omega}_i^{\text{dl}}}{\tau}\right) \leq \tau P_i^{\text{dl}}, \; i \in \mathcal{N}_R, \tag{19d}$$

$$\text{Re}(\mathbf{h}_k^H \tilde{\mathbf{v}}_k) \geq 0, \; k \in \mathcal{N}_U, \tag{19e}$$

$$(1h), (8), (9), (10), (11), (15), (17), (18),$$

where $\mathcal{A} \triangleq \{\tilde{\mathbf{v}}, \tilde{\boldsymbol{\rho}}, \tilde{\boldsymbol{\Omega}}^{\text{dl}}, \tilde{\boldsymbol{\Omega}}^{\text{ul}}, \boldsymbol{\alpha}, \tau, \boldsymbol{\mu}, \boldsymbol{\theta}, \boldsymbol{e}\}$ with $\boldsymbol{\mu} \triangleq \{\mu_k \text{ for } k \in \mathcal{N}_U\}$ and the constraints (19d) and (19e) are equivalent to the constraints (1f) and (1g), respectively. Note that convex problem (19) can be solved by exploiting convex solvers such as CVX [23].

Now, we summarize the proposed SCA process for problem (1). We first initialize the set $\mathcal{A}^{(0)}$ satisfying the constraints (1b)–(1h), (7), (13), (14), (19b) and (19c). Next, at the t-th iteration, we update the optimization set $\mathcal{A}^{(t+1)}$ as a solution to the convex problem in (19). Then, this procedure is repeated until convergence. It has been verified that this SCA algorithm converges to a locally optimal point [12].

V. Numerical Results and Conclusions

In this section, we provide numerical results to evaluate the performance of the proposed algorithm. For the simulations, we set $N_R = 2$, $N_U = 3$, $M = 4$, $\sigma_d^2 = \sigma_u^2 = \sigma_C^2 = -80$ dBm and $E_{S,k}^{\text{ul}} = 50$ nJ. The non-linear EH parameters are fixed as $\delta_k = 150$, $\epsilon_k = 0.014$, and $M_k = 0.024$ for $k \in \mathcal{N}_U$ [20]. Also, the downlink transmit power at the RRHs is given by $P_i^{\text{dl}} = P^{\text{dl}}, \forall\, i \in \mathcal{N}_R$, and each RRH has the same fronthaul capacity C, i.e., $C_i = C$, $\forall\, i \in \mathcal{N}_R$. For simplicity, we assume that the RRHs and the UEs are located on a one-dimensional line.

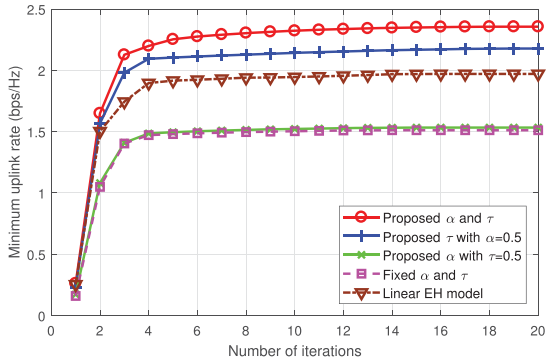

Fig. 2. Convergence behavior of the proposed algorithm.

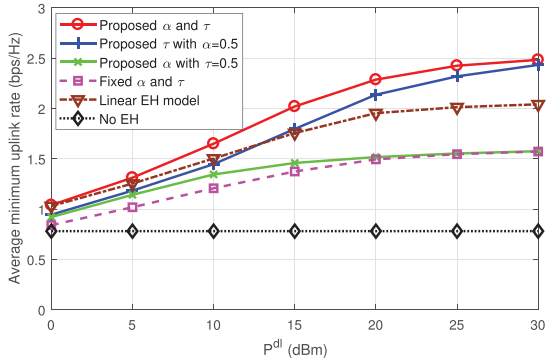

Fig. 3. Average minimum uplink rate with respect to P^{dl} for a C-RAN system with $R_{\min}^{\text{dl}} = 0.5$ bps/Hz and $C = 5$ bps/Hz.

The RRHs are apart from each other by 10 m and UE 2 is halfway between the RRHs. UE 1 and UE 3 are located at 5 m the left of RRH 1 and the right of RRH 2, respectively. We consider the Rayleigh fading channels $\mathbf{h}_{k,i}$ and $\mathbf{g}_{k,i}$ with the path-loss model given as $c_0(\frac{d_{k,i}}{d_0})^{-\beta}$, where c_0 denotes a constant attenuation at the reference distance $d_0 = 1$ m as $c_0 = -20$ dB, $d_{k,i}$ indicates the distance between UE k and RRH i, and $\beta = 3$ represents the path-loss exponent [10].

We compare our proposed algorithm with the following baseline schemes.

- *Fixed α and τ*: The proposed algorithm is executed with the fixed uniform PS ratios $\alpha_k = 0.5, \forall k$, and time allocation factor $\tau = 0.5$.
- *Linear EH model*: The proposed algorithm is performed by replacing $E_{H,k}^{\text{ul}}(\mathbf{v}, \boldsymbol{\Omega}^{\text{dl}}, \alpha_k, \tau)$ in (1e) with the linear EH model $\eta\tau P_{H,k}^{\text{ul}}(\mathbf{v}, \boldsymbol{\Omega}^{\text{dl}}, \alpha_k)$, where $\eta = 0.7$ is the energy conversion efficiency at the UEs.
- *No EH* : The UEs use all received signal power for decoding the information without EH, i.e., $\alpha_k = 1, \forall k$, (conventional uplink C-RAN).

In Fig. 2, we plot the convergence behavior of the proposed algorithm with $R_{\min}^{\text{dl}} = 0.5$ bps/Hz, $C = 5$ bps/Hz and $P^{\text{dl}} = 20$ dBm. We can see that the proposed algorithm converges to a stable point for all schemes. In addition, the minimum uplink rate of the proposed algorithms converges within 10 iterations.

Fig. 3 plots the average minimum uplink rate with respect to the downlink power P^{dl} with $R_{\min}^{\text{dl}} = 0.5$ bps/Hz and $C = 5$ bps/Hz. It is observed that the proposed algorithm always outperforms the baseline schemes. Since the uplink fronthaul capacity limitations are the performance bottleneck, the performance of the schemes with the fixed τ is saturated at high P^{dl}. In contrast, the performance of the schemes with the proposed τ does not get saturated at high P^{dl}, since the BBU allocates more time to the uplink to overcome the uplink fronthaul

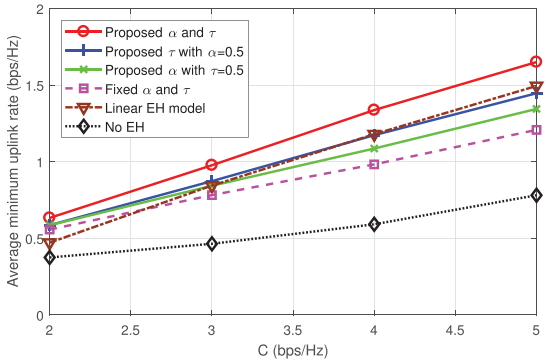

Fig. 4. Average minimum uplink rate with respect to C for a C-RAN system with $R_{\min}^{\mathrm{dl}} = 0.5$ bps/Hz and $P^{\mathrm{dl}} = 10$ dBm.

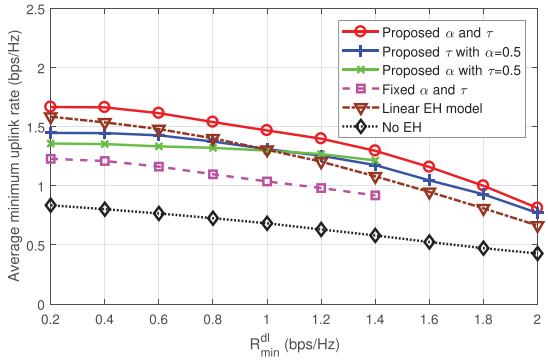

Fig. 5. Average minimum uplink rate with respect to $R_{\min}^{\mathrm{dl}}$ for a C-RAN system with $C = 5$ bps/Hz and $P^{\mathrm{dl}} = 10$ dBm.

capacity limitations. In addition, it is shown that due to the uplink transmit power mismatch caused by the impractical linear EH model, the performance gap between the schemes based on the non-linear and linear EH models becomes larger as $P_{\min}^{\mathrm{dl}}$ grows.

In Fig. 4, we illustrate the average minimum uplink rate in terms of the fronthaul capacity C with $R_{\min}^{\mathrm{dl}} = 0.5$ bps/Hz and $P^{\mathrm{dl}} = 10$ dBm. We can see that the advantages of the proposed algorithm are more pronounced for a large C. Also, all schemes that leverage EH exhibit that the average minimum uplink rate increases more rapidly with C as compared to the no EH scheme. Thus, the figure suggests that the EH technique is quite effective to improve the performance of a C-RAN system with battery-limited UEs.

Fig. 5 depicts the average minimum uplink rate with respect to $R_{\min}^{\mathrm{dl}}$ with $C = 5$ bps/Hz and $P^{\mathrm{dl}} = 10$ dBm. We can check that the proposed algorithm provides better performance compared to the baseline schemes. Also note that the schemes with the fixed τ cannot satisfy the required minimum downlink rate $R_{\min}^{\mathrm{dl}}$ greater than 1.4 bps/Hz. Throughout the numerical results, we have confirmed that the proposed algorithm outperforms the conventional schemes. Development of new signal processing strategies for a wireless powered C-RAN under more practical EH models (e.g., [18]) will be an important future work.

REFERENCES

[1] S.-H. Park, O. Simeone, O. Sahin, and S. Shamai (Shitz), "Fronthaul compression for cloud radio access networks: Signal processing advances inspired by network information theory," *IEEE Signal Process. Mag.*, vol. 31, no. 6, pp. 69–79, Nov. 2014.

[2] O. Simeone, A. Maeder, M. Peng, O. Sahin, and W. Yu, "Cloud radio access network: Virtualizing wireless access for dense heterogeneous systems," *J. Commun. Netw.*, vol. 18, pp. 135–149, Apr. 2016.

[3] S.-H. Park, K.-J. Lee, C. Song, and I. Lee, "Joint design of fronthaul and access links for C-RAN with wireless fronthauling," *IEEE Signal Process. Lett.*, vol. 23, no. 11, pp. 1657–1661, Nov. 2016.

[4] J. Kim, S.-H. Park, O. Simeone, I. Lee, and S. Shamai (Shitz), "Joint design of digital and analog processing for downlink C-RAN with large-scale antenna arrays," in *Proc. IEEE Int. Workshop Signal Process. Adv. Wireless Commun.*, Jul. 2017, pp. 1–5.

[5] R. Zhang and C. K. Ho, "MIMO broadcasting for simultaneous wireless information and power transfer," *IEEE Trans. Wireless Commun.*, vol. 12, no. 5, pp. 1989–2001, May 2013.

[6] A. A. Nasir, H. D. Tuan, D. T. Ngo, T. Q. Duong, and H. V. Poor, "Beamforming design for wireless information and power transfer systems: Receive power-splitting versus transmit time-switching," *IEEE Trans. Commun.*, vol. 65, no. 2, pp. 876–889, Feb. 2017.

[7] H. Ju and R. Zhang, "Throughput maximization in wireless powered communication networks," *IEEE Trans. Wireless Commun.*, vol. 13, no. 1, pp. 418–428, Jan. 2014.

[8] H. Kim, H. Lee, M. Ahn, H.-B. Kong, and I. Lee, "Joint subcarrier and power allocation methods in full duplex wireless powered communication networks for OFDM systems," *IEEE Trans. Wireless Commun.*, vol. 15, no. 7, pp. 4745–4753, Jul. 2016.

[9] H. Lee, K.-J. Lee, H.-B. Kong, and I. Lee, "Sum-rate maximization for multiuser MIMO wireless powered communication networks," *IEEE Trans. Veh. Technol.*, vol. 65, no. 11, pp. 9420–9424, Nov. 2016.

[10] J. Kim, H. Lee, C. Song, T. Oh, and I. Lee, "Sum throughput maximization for multi-user MIMO cognitive wireless powered communication networks," *IEEE Trans. Wireless Commun.*, vol. 16, no. 2, pp. 913–923, Feb. 2017.

[11] A. A. Nasir, D. T. Ngo, X. Zhou, R. A. Kennedy, and S. Durrani, "Joint resource optimization for multicell networks with wireless energy harvesting relays," *IEEE Trans. Veh. Technol.*, vol. 65, no. 8, pp. 6168–6183, Aug. 2016.

[12] V.-D. Nguyen, T. Q. Duong, H. D. Tuan, O.-S. Shin, and H. V. Poor, "Spectral and energy efficiencies in full-duplex wireless information and power transfer," *IEEE Trans. Commun.*, vol. 65, no. 5, pp. 2220–2233, May 2017.

[13] Z. Chen, L. X. Cai, Y. Cheng, and H. Shan, "Sustainable cooperative communication in wireless powered networks with energy harvesting relay," *IEEE Trans. Wireless Commun.*, vol. 16, no. 12, pp. 8175–8189, Dec. 2017.

[14] Z. Chen, Z. Chen, L. X. Cai, and Y. Cheng, "Energy-throughput tradeoff in sustainable cloud-RAN with energy harvesting," in *Proc. IEEE Int. Conf. Commun.*, May 2017, pp. 1–6.

[15] Z. Chen, Z. Chen, L. X. Cai, and Y. Cheng, "Optimal beamforming design for simultaneous wireless information and power transfer in sustainable cloud-RAN," *IEEE Trans. Green Commun. Netw.*, vol. 2, no. 1, pp. 163–174, Mar. 2018.

[16] C. Qin, W. Ni, H. Tian, and R. P. Liu, "Fronthaul load balancing in energy harvesting powered cloud radio access networks," *IEEE Access*, vol. 5, pp. 7762–7775, 2017.

[17] T. Le, K. Mayaram, and T. Fiez, "Efficient far-field radio frequency energy harvesting for passively powered sensor networks," *IEEE J. Solid-State Circuits*, vol. 43, no. 5, pp. 1287–1302, May 2008.

[18] J. Guo and X. Zhu, "An improved analytical model for RF-DC conversion efficiency in microwave rectifiers," in *Proc. IEEE MTT-S Int. Microw. Symp. Dig.*, Jun. 2012, pp. 1–3.

[19] E. Boshkovska, D. W. K. Ng, N. Zlatanov, and R. Schober, "Practical non-linear energy harvesting model and resource allocation for SWIPT systems," *IEEE Commun. Lett.*, vol. 19, no. 12, pp. 2082–2085, Dec. 2015.

[20] E. Boshkovska, D. W. K. Ng, N. Zlatanov, A. Koelpin, and R. Schober, "Robust resource allocation for MIMO wireless powered communication networks based on a non-linear EH model," *IEEE Trans. Commun.*, vol. 65, no. 5, pp. 1984–1999, May 2017.

[21] A. Al-Shuwaili, O. Simeone, A. Bagheri, and G. Scutari, "Joint uplink/downlink optimization for Backhaul-limited mobile cloud computing with user scheduling," *IEEE Trans. Signal Inf. Process. Netw.*, vol. 3, no. 4, pp. 787–802, Dec. 2017.

[22] A. E. Gamal and Y.-H. Kim, *Network Information Theory*. Cambridge, U.K.: Cambridge Univ. Press, 2012.

[23] M. Grant and S. Boyd, *CVX: Matlab Software for Disciplined Convex Programming*. Version 2.1, 2017. [Online]. Available: http://cvxr.com/cvx